# A Study of Layered Structural Configurations as Thermal and Impact Shielding of Lunar Habitats

Jeffrey T. Steiner[1] and Ramesh B. Malla, Ph.D., F.ASCE[2]

[1]Graduate Assistant, Dept. of Civil and Environmental Engineering, Univ. of Connecticut, Storrs, CT. Email: jeffrey.steiner@uconn.edu
[2]Professor, Dept. of Civil and Environmental Engineering, Univ. of Connecticut, Storrs, CT. Email: Ramesh.Malla@uconn.edu

## ABSTRACT

The focus of this study is the analysis of a proposed multilayer material configuration as lunar habitat shielding so as to assess its ability to resist temperature extremes and impact. In order to resist this environmental hazard, the analysis will compare various configurations of potential shielding layers using both in-situ resource utilization (ISRU) and Earth-based materials. The technology for implementation of in-situ resources in construction is developing, though not yet able to produce a functional lunar habitat. As the lunar infrastructure is developed, ISRU techniques for manufacturing and construction may become more viable. Therefore, both types of materials are considered due to potential for application towards both near-term and long-term commencements of habitat construction. The thermal analysis in this paper utilizes the nonlinear heat equation to produce a depth-dependent temperature gradient from the habitat exterior to the interior that changes continuously with time during the lunar diurnal cycle. Static loading conditions meant to simulate the impact force of a 77.9 g meteorite were used to analyze the ability of a proposed multilayer shielding configuration to resist impact. A thermal stress analysis was performed to observe the effects of heat transfer through the proposed multilayer configuration. The results of this study should be useful in determining the potential for implementation of efficient shielding layers for the initial lunar base.

## INTRODUCTION

The next logical step in the advancement of manned space exploration is a return to the Moon for an extended period of time. The Moon presents a plethora of opportunities for testing advancements in technologies related to spaceflight and extraterrestrial habitation, as well as the ability to act as a low-gravity origin point for further human exploration throughout the solar system (NASA, 2018). The establishment of a long-term human footprint on the Moon is dependent on the ability of the space industry to overcome the challenges that will be presented during future attempts to inhabit the lunar surface. The lunar environment presents a multitude of technical challenges to be overcome that include but are not restricted to: a hard vacuum, lack of substantial atmosphere, susceptibility to multiple forms of dangerous cosmic radiation, potential for micrometeoroid impacts at hypervelocity, and a broad range of temperature extremes (Malla & Brown, 2015). The last of these, temperature extremes, is the main focus of this study, though the construction of a safe lunar habitat requires a design that addresses all of these technical challenges in a cost-effective manner. For this reason, others factors such as meteorite impact and the effects of cosmic radiation have been considered in the design of the proposed Multi-Layer shielding.

## METHODOLOGY

The governing equation for the temperature as determined on the lunar surface is given by the one-dimensional heat conduction equation (Malla and Brown, 2015):

$$kV \frac{\delta^2 T(X,t)}{\delta X^2} - Mc \frac{\delta T(X,t)}{\delta t} = \dot{q}_{out}(X,t) - \dot{q}_{in}(X,t) \tag{1}$$

$$-Mc \frac{\delta T(t)}{\delta t} = \dot{q}_{out}(X,t) - \dot{q}_{in}(X,t) = (\dot{q}_{nbb} + \dot{q}_r) - (\dot{q}_s + \dot{q}_i) \tag{2}$$

Where, $k$ is the thermal conductivity of the material, $V$ represents the volume of the material, $t$ is the time, $X$ is the depth in the material, $T$ represents the temperature at depth $X$ at time $t$, $M$ is the mass of the material, and $c$ signifies the specific heat of the material. The two temperature-inclined variables, thermal conductivity and specific heat, can be described as a measure of a materials ability to conduct heat, and the amount of heat energy per unit mass required to raise the temperature of the material by one degree Celsius. A comprehensive diagram of the input and output behavior of the system can be seen in Figure 1.
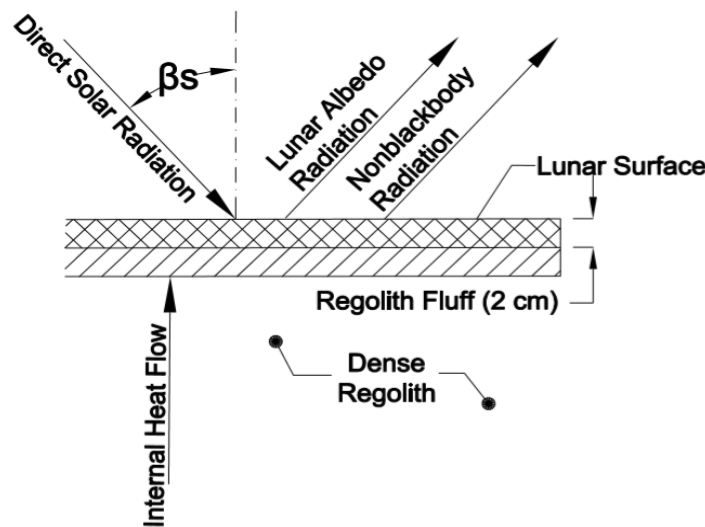


**Figure 1 - Diagram showing the input and output terms for determination of the Lunar surface temperature**

The surface temperature can be determined by removing the term that takes depth into account, and solving the Equation (2). Equation (2) determines the derivative of temperature with respect to time, which excludes the term associated with depth.

In order to solve for the surface temperature on the lunar surface, an initial temperature must be defined. Steady state is a particularly useful special case within thermodynamics in which there is no dependence of the system on time. With respect to the lunar surface, this definition leads to the simplification of Eq. (1) by setting the left side differential equal to zero. The resulting expression simply states that during steady state, the incoming heat sources, $\dot{q}_{in}(X,t)$, must be equal in magnitude to the outgoing heat sinks, $\dot{q}_{out}(X,t)$. This results in no net gain or

loss of heat within the system, assuming that ample time is provided for steady state to be reached. Eq. (3) and Eq. (4) show the steady state relationship between the applicable heat sources for the lunar surface.

$$(\dot{q}_s + \dot{q}_i) = (\dot{q}_{nbb} + \dot{q}_r) \tag{3}$$

$$G_{s,max}A + a_s G_i = A\varepsilon\sigma T_s^4 + (1 - a_s)G_{s,max}A \tag{4}$$

By solving this relationship for the unknown variable $T$ using the values shown in Table 1, the steady state temperature for the lunar surface can be found. This value will later serve as a boundary condition and initial data point for the numerical analysis performed to determine the temperature of the surface throughout the entire lunar cycle. The Heat equation (Eq. 2) with the above input and output terms was solved to produce temperature values with respect time. The results of that solution can be seen in Figure 2, which corresponds to the surface temperature of an area located directly on the lunar surface. The inclusion of a $T^4$ term on the right-hand side of Eq. (1) and Eq. (2), as a result of the non-blackbody radiation term, creates a highly non-linear equation. In this case, the 4th-order Runge-Kutta method was used (Malla and Brown, 2015).
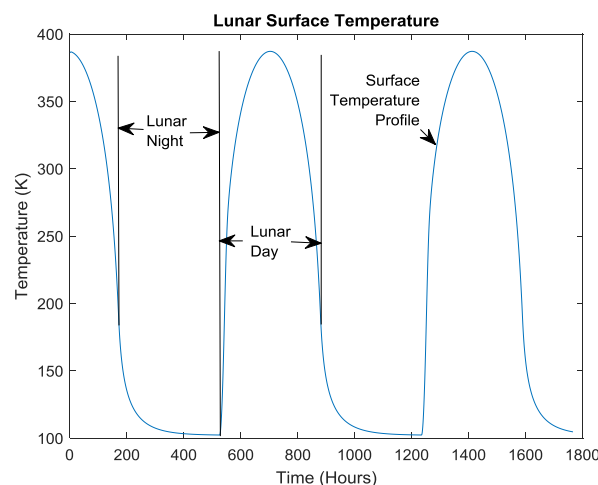


**Figure 2 - Lunar surface temperature for a flat ground surface comprised of lunar regolith (Malla and Brown, 2015)**

The surface temperature determined is applicable to the lunar regolith surface. The habitat surface temperature must account for the additional input of albedo from the lunar surface. In this study, regular strength concrete was chosen as a control material for comparison of the effectiveness of layered configurations. Concrete has material properties that vary from those of lunar regolith and, as such, produce a differing temperature profile. The material properties used for concrete, aluminum, and lunar regolith have been briefly summarized in Table 1.

In addition to the change of material properties, determining the temperature on any proposed habitat surface requires additional input, as displayed in Figure 3. This additional input comes in the form of the albedo reflected off of the lunar surface and onto the raised habitat surface. This albedo input value is multiplied by the absorptivity of the dome surface material to determine the amount of energy that is absorbed from the albedo.
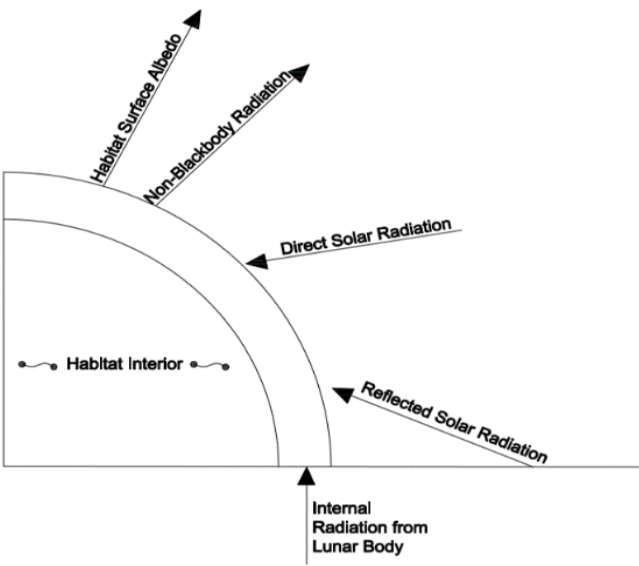
**Figure 3 - Diagram showing input and output for the Habitat Surface Temperature Analysis**

**Table 1 - General Material Properties used in the Structural Thermal Model**

| Material Properties used in the Thermal Analysis | | | | |
|---|---|---|---|---|
| Material Property | Concrete | Regolith | Aluminum | Units |
| | Value | Value | Value | |
| Absorptivity | 0.6 | 0.13 | 0.14 | - |
| Reflectivity | 0.4 | 0.87 | 0.86 | - |
| Emissivity | 0.85 | 0.97 | 0.9 | - |
| Thermal Conductivity | 1 | *** | 240 | W/m-K |
| Specific Heat | 1000 | *** | 910 | J/kg-K |
| Density | 1500 | 1000-2000 | 2712 | kg/m$^3$ |
| Stefan-Boltzmann Constant | 5.6704 x 10$^{-8}$ | 5.6704 x 10$^{-8}$ | 5.6704 x 10$^{-8}$ | W/m$^2$-K$^4$ |
| Solid Conductivity | - | 0.0093 | - | W/m-K |
| $\chi$ | - | 0.073 | - | - |

*** - Varies with temperature, defined in Malla and Brown (2015)

Having considered the additional albedo input term, the resulting structural surface temperature profile is as shown in Figure 4. For purposes of consistency with the control material, all configurations within this study use the Concrete Structure Surface Temperature.

© ASCE

*Temperature through Wall Thickness as a Function of Time and Depth*

The determination of the temperature gradient throughout the wall thickness is governed by the following partial differential equation:

$$kV\frac{\delta^2 T(X,t)}{\delta X^2} - Mc\frac{\delta T(X,t)}{\delta t} = 0 \tag{5}$$

$$\frac{dT}{dt} = \alpha(\dot{q}_{in} - \dot{q}_{out}) \tag{6}$$

where
$$\alpha = \frac{k}{\rho c} \tag{7}$$

Equation (5) is a second-order partial differential equation that requires two surface conditions as described below.

At Exterior Surface: Eq. (2) represents the exterior surface. This equation is simplified in Eq. (6), and the material property inputs are defined in Eq. (7) where $\alpha$ is the thermal diffusivity of the material. In Eq. (6), the subscripts "in" and "out" refer to the sums of the inputs and outputs, respectively.

At Interior Surface: The temperature is kept at a reasonable room value of T = 293.15 Kelvin (Room Temperature or 20 °C) (8)

In addition, in order to find the solution of Eq. (5), one initial condition must be applied. An initial condition of 293.15 Kelvin was chosen for the entire structure, as this temperature is representative of a typical value for room temperature or 20 °C. This initial temperature was applied to all nodal analysis points throughout the wall thickness. The boundary condition applied on the exterior habitat surface for all time *t* can be seen in Figure 4. The method of solution used was the Forward-Euler Method of Numerical Approximation (Edwards et al.*,* 2008). This method was used to develop code using the software MATLAB to perform the heat transfer analysis. The input for this MATLAB program included material properties, using the values displayed in Table 1, as well as the definition of parameters such as wall thickness, and number of elements into which the wall would be separated for analysis (as will be given below).
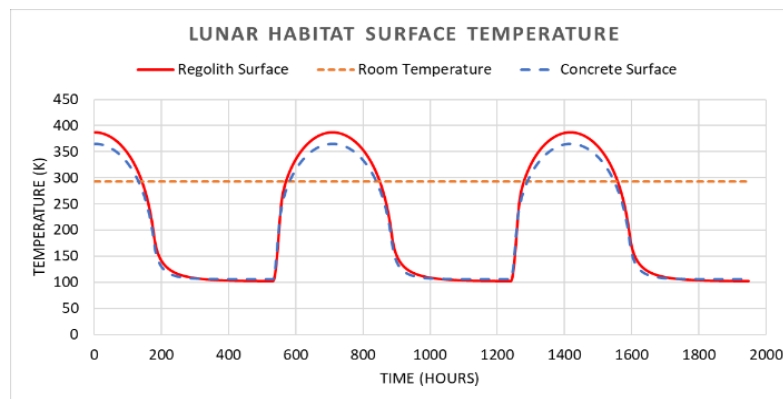


**Figure 4 - Lunar Habitat Concrete Surface Temperature & Room Temperature Comparison**

© ASCE

## HEAT TRANSFER RESULTS

Examination of selected material resistance to both thermal and impact loads requires determination of stresses placed on the materials by those loads. In order to determine these stresses, a finite element model was analyzed. A two-dimensional plate, measuring 40 cm square, was used to analyze both the concrete control and the layered configurations. A heat transfer analysis, using the same conditions as applied in the MATLAB analysis, was performed using the software ABAQUS, and compared to the MATLAB results. The result of the ABAQUS model heat transfer analysis is shown in Figure 5, and is included to display the limited penetration of the external temperature, even after long periods of time. The full comparison of temperature time histories between ABAQUS and MATLAB can be seen in Figure 6, which shows the accuracy of the MATLAB code in calculating heat transfer results.
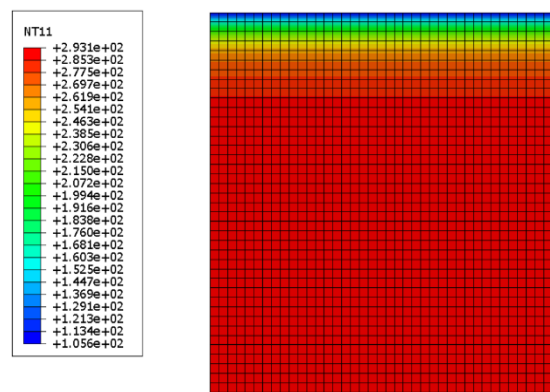


**Figure 5 – ABAQUS Heat Transfer model nodal temperature contour plot after 1,948 hours or 3 Lunar days for Concrete**

*Material Comparison*

Using the methodology discussed, three material configurations were analyzed for their effectiveness in insulating against heat transfer with the Lunar Environment. For this study, the materials considered were Portland Cement Concrete, Laser Sintered Regolith, and a proposed Multi-Layer configuration.

The Multi-Layer configuration proposed has drawn inspiration from existing shielding configurations in use on the International Space Station (ISS). The shielding on the ISS utilizes a variety of materials meant to mitigate the potential effects of temperature, radiation, and micrometeorite impact. A diagram of the ISS configuration can be seen in Figure 7.

The Multi-Layer configuration proposed in this study utilizes the same format of a thermal layer on the exterior, followed by alternating impact layers. The Multi-Layer configuration includes the following materials:

- Kevlar – Aramid 49
- Silica Aerogel Vacuum Insulation Panel
- Aluminum Foam
- Al2017-T4 Aluminum Alloy
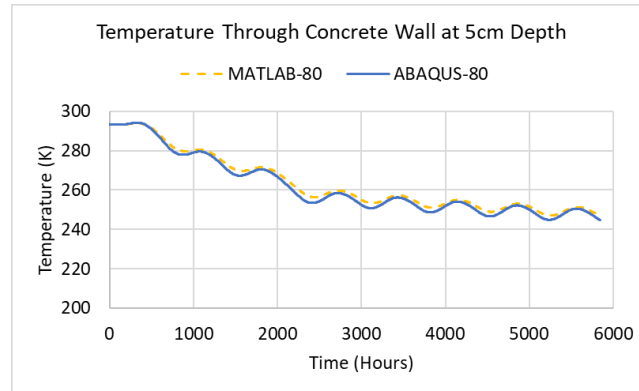- Ultra-High Molecular Weight Polyethylene (UHMWPE)

© ASCE

**Figure 6 – Temperature Time History Comparison for Regolith Concrete of MATLAB and ABAQUS models using data from a depth of 5cm through the wall**
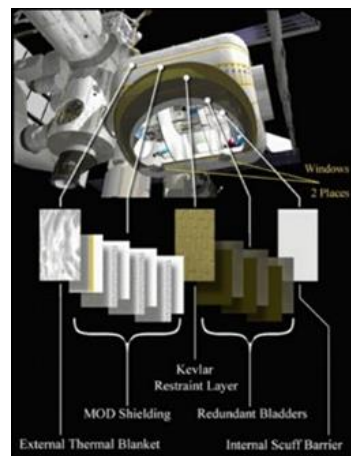


**Figure 7 – ISS Shielding Detail (From NASA, 2001)**

So as to examine the contribution of each individual layer within the Multi-Layer configuration, each material was tested with the same heat transfer analysis in MATLAB. The results of this testing can be seen in Figure 8. The Silica Aerogel Vacuum Insulation Panel showed the greatest resistance to heat transfer, as evidenced by its temperature range of ~235 K-~305 K at 1 cm in depth through the material as seen in Figure 8a. The UHMWPE also performs well in reducing heat transfer, as its range of temperature values was slightly greater, at ~205 K-~315 K, than the Aerogel. Both of these materials significantly outperform the Aluminum-based materials in heat transfer, as can be observed in Figure 8b. For this reason, the aluminum foam and aluminum plate can be considered to provide no benefit in resisting heat transfer, and should be considered as impact shielding only. The Multi-Layer configuration, as outlined in Figure 10, was analyzed alongside 40 cm thick plates of Portland Cement Concrete (PCC) and Laser-Sintered Regolith, both of which are common materials suggested in In-Situ Resource Utilization plans for Lunar Construction. The results of this analysis are also presented in Figure 8, showing that the Multi-Layer configuration outperforms an equivalent thickness of Concrete or Laser-Sintered Regolith with respect to heat transfer.
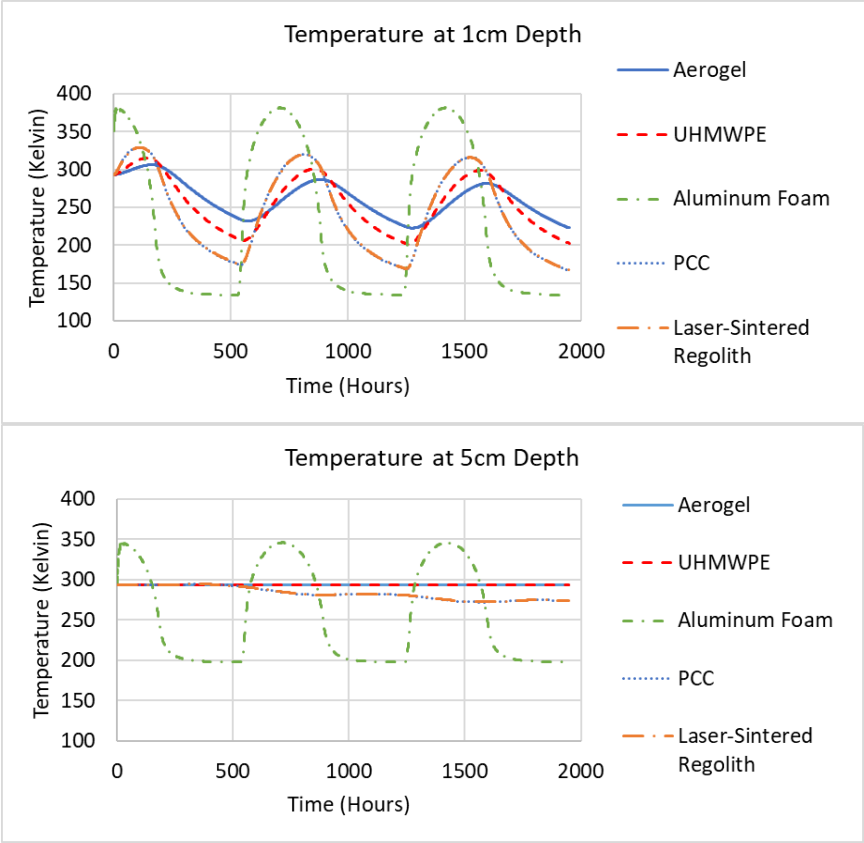
**Figure 8 – Temperature change over time for materials within the Multi-Layer configuration compared to ISRU options at a) 1cm depth and b) 5cm depth**
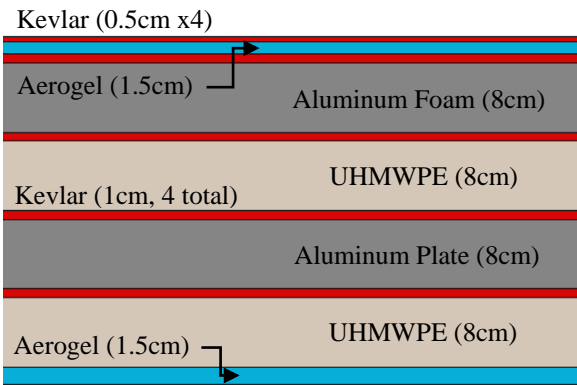


**Figure 9 – Proposed Multi-Layer configuration throughout wall thickness**

## Static Loading Analysis

The results of the heat transfer analysis show that the Multi-Layer configuration is a viable alternative to proposed ISRU methods from a temperature standpoint. The proposal of a layered configuration for study required consideration of multiple hazards that would be faced in the

Lunar environment. Studies have been performed to determine performance of UHMWPE as shielding against cosmic radiation (Zhong et al., 2009; Seetala et al., 2014) which governed the decision to include this material in the wall thickness configuration presented in Figure 9 of this study. Previous studies have been performed (Ryan & Christiansen, 2009) on the efficiency of open-cell aluminum foam in resisting hypervelocity impact. A combination of an upper layer of open-cell aluminum foam and a lower layer of Al2017-T4 aluminum plate was chosen to provide the majority of the structural stiffness within the Multi-Layer configuration wall. For this reason, an elastic, static loading analysis was performed in ABAQUS on a simply-supported beam to determine the ability of the Multi-Layer configuration, and the aluminum layers in particular, to resist impact forces, as noted below.

The impact event considered involved a meteorite with a mass of 77.9 grams and a velocity of 33.4 km/s. This coincided with impact events observed as the Earth-Moon system encountered annual meteor shower systems (Suggs et al., 2014). The kinetic energy of this particular meteorite, which amounted to approximately $4.36 \times 10^7$ Joules of energy, was used, along with the principles of beam-bending due to a central point load for a simply-supported beam and the principle of the work-energy balance, to determine the impact force of the meteorite (Malla & Gionet, 2011). In this case, the work-energy balance is given by Equation (9).

$$Kinetic\ Energy\ (KE) = Force\ (P) * Distance\ (\Delta) \qquad (9)$$

Regarding mechanical properties of the Multi-Layer configuration, the values for Young's Modulus (E = 37.69 GPa) and moment of inertia (I = 1.44548 x $10^{-6}$ m$^4$) (and Inertia, respectively) were established through the calculation of weighted values using the respective values of each layer in the Multi-Layer configuration and the thickness of each layer (Brahma & Mukherjee, 2010). Using the principle outlined in Equation (9), the meteorite was determined to have an equivalent static impact force of approximately 17,208 kN.
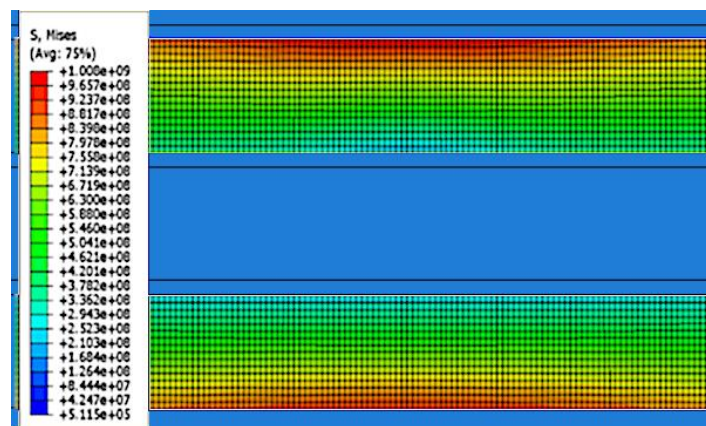


**Figure 10 – Von Mises stress (Pascals) measured in the layers of aluminum foam (upper) and aluminum plate (lower) within the Multi-Layer simply-supported beam under 17,208 kN load.**

The effect of the impact force is analyzed as an equivalent static load using ABAQUS, as described below. This force was applied as a concentrated load at the midspan of a 4-meter long, 0.4-meter deep 2-dimensional beam composed of the Multi-Layer configuration in consideration.

The beam was analyzed to determine stress in each layer, with the primary concern being the stress developed within the aluminum layers, specifically included to withstand impact. The results of this stress analysis within the two layers of aluminum can be seen in Figure 10, with the surrounding non-aluminum layers shaded in blue and displaying no stress results.

It can be seen that the stress observed within the aluminum foam layer exceeds the typical yield strength of ~3.5 MPa (Deshpande & Fleck, 1999). It is for this reason that the lower aluminum plate, comprised of aerospace-grade Al2017-T4 aluminum, has been provided. The plate exceeds the yield strength of 276 MPa for the material through approximately 90% of the thickness. The ultimate strength of the material has been measured as 427 MPa, below which lies ~45% of the material thickness (Holt, 1996). Therefore, the plastic deformation of the multi-layer plate is expected to occur, but total failure is not anticipated.

## DOME STRUCTURE

In order to begin to assess the practicality of the Multi-Layer configuration as an alternative option for Lunar construction, a 2-dimensional cross-section of a proposed dome structure (Figure 11b) made of the layered wall configuration shown in Figure 9 has been chosen for structural analysis, utilizing the ABAQUS CAE finite element (FE) code. The proposed dome has an interior diameter of 2.5 meters, and an exterior diameter of 2.9 meters. These dimensions provide the necessary 0.4 meters of wall thickness to match the plate cross section which was analyzed for the heat transfer portion of this study. The FE model of the structure has a mesh resolution of 80 element layers throughout the thickness of the habitat wall and a total of 16,766 elements across the entire system.
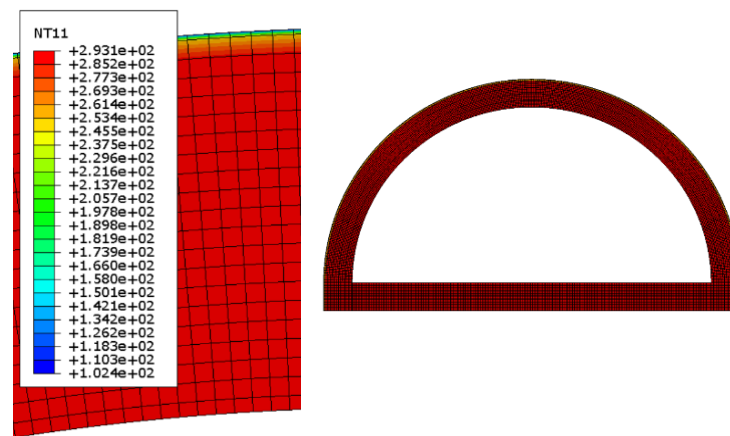


**Figure 11 – a) Heat transfer results (3 Lunar days) at the top of the dome and b) across the entire dome for the Multi-Layer configuration**

The Multi-Layer heat transfer analysis was performed on the dome structure, producing the same results as expected, and can be seen in Figure 11 (a, b). The outer layer of Silica Aerogel Vacuum Insulation Paneling resists most of the potential heat transfer, maintaining a thin depth of penetration for thermal effects from the exterior environment. If, however, an impact scenario was to occur, it is assumed that this layer would be damaged and unable to function properly,

resulting in a deeper penetration for the thermal effects due to exposure to the exterior environment. The heat transfer results were used to calculate thermal stresses in the material of the Multi-Layer configuration. The results of this thermal stress analysis showed that the extreme temperature fluctuations in the outermost regions of the material produced small amounts of stress in comparison to material yield stress limits. This might be due to low stiffness of some layers and some others being open-cell configuration.

## CONCLUSIONS

In this study, the viability of a Multi-Layer configuration comprised of common materials used on Earth as a shield against temperature change and meteorite impact on the Lunar surface was examined. The thermodynamics heat transfer analysis to determine temperature variation as a function of depth and time was performed using an in-house code developed in MATLAB utilizing the Forward-Euler Method, and verified with a comparison to the heat transfer results from ABAQUS finite element code. The Multi-Layer configuration was comprised of Kevlar Aramid-49 fabric, Silica Aerogel Vacuum Insulation Panels, Open-Cell Aluminum Foam, AL2017-T4 aluminum alloy, and Ultra-High Molecular Weight Polyethylene. This Multi-Layer configuration outperformed two frequently proposed materials for In-Situ Resource Utilization (ISRU): Portland Cement Concrete and Laser-Sintered Regolith. The inclusion of the aerogel layers provided enough heat resistance to outperform the ISRU materials while limiting the amount of weight added to the structure, an important factor in consideration for extraterrestrial construction.

The ability of the aerogel layers to outperform the thermal resistance of ISRU materials while adding little extra weight allows for the inclusion of other layers to address other aforementioned hazards of the Lunar environment. The proposed layers of aluminum foam and aluminum plate are provided as a potential solution for meteorite impact resistance, while the UHMWPE is able to provide some resistance to harmful ionizing radiation.

The analysis methodology utilized provides an ability to examine many different shielding configurations, including ISRU or the usage of terrestrial materials. This method allows a designer to establish a reliable analysis of structural thermal performance, applicable to any proposed materials.

## ACKNOWLEDGEMENTS

## REFERENCES

Deshpande, V. S., and N. A. Fleck. (1999)."Multi-axial yield of aluminium alloy foams."
    MetFoam'99 Proceedings. Fraunhofer Institute, Bremen, Germany. Pp 247-254.

Edwards, C. H., Penney, D. E., and Calvis, D. (2008). *Elementary differential equations with boundary value problems*. Pearson Education, Inc., Upper Saddle River, NJ, pp 430-439.

Holt, J. M. (1996). *Structural alloys handbook*, (C. Y. Ho, Ed.), CINDAS/Purdue University, West Lafayette, IN.

Malla, R. B., and Brown, K. (2015). "Determination of temperature variation on lunar surface and subsurface for habitat analysis and design," *Acta Astronautica*, Vol. 107, Feb-Mar, 196-207.

Malla, R. B., and. Gionet, T.G. (2011). "Dynamic response of a pressurized frame-membrane lunar structure with regolith cover subjected to impact load." *Journal of Aerospace Engineering* 26(4). 855-873.

NASA, (2001). "Home, space home" NASA science and technology directorate. Marshall Space Flight Center, Huntsville, AL. (online: https://science.nasa.gov/science-news/science-at-nasa/2001/ast14mar_1/)(Accessed: May 15, 2019).

NASA, (2018). "Strategic goal 2: Extend human presence deeper into space and to the moon for sustainable longterm exploration and utilization." NASA *strategic plan* 2018. National Aeronautics and Space Administration (NASA), Washington, D.C. 16-21.

Ryan, S., and Christiansen, E.L. (2010). "Honeycomb vs. foam: Evaluating potential upgrades to ISS module shielding," *Acta Astronautica*. Vol. 67, Oct-Nov, 818-825.

Seetala, N., et al. (2014). "Positron lifetime studies of irradiated ultra-high molecular weight polyethylene and composites made of Martian regolith," *Materials Science Forum*, Vols. 783-786, May, 1585-1590.

Suggs, R.M., et al. (2014). "The flux of kilogram-sized meteoroids from lunar impact monitoring" *Icarus*, Vol. 238, May, 23-36.

Zhong, W.H., et al. (2008). "Cosmic radiation shielding tests for UHMWPE fiber/nano-epoxy composites" *Composites Science and Technology*. Vol. 69, 2093-2097.